Polymer 50 (2009) 3211–3219

Contents lists available at ScienceDirect

Polymer

journal homepage: www.elsevier.com/locate/polymer

Interactions between silica nanoparticles and an epoxy resin before and during network formation

Jörg Baller*, Nora Becker, Markus Ziehmer, Matthieu Thomassey, Bartosz Zielinski, Ulrich Müller, Roland Sanctuary

University of Luxembourg, 162a avenue de la Faïencerie, L-1511 Luxembourg, Luxembourg

ARTICLE INFO

Article history:
Received 2 April 2009
Received in revised form
11 May 2009
Accepted 13 May 2009
Available online 20 May 2009

Keywords:
Nanocomposite
Thermoset
Epoxy

ABSTRACT

In polymer nanocomposites, interactions between filler particles and matrix material play a crucial role for their macroscopic properties. Nanocomposites consisting of varying amounts of silica nanoparticles and an epoxy resin based on diglycidyl ether of bisphenol-A (DGEBA) have been studied before and during network formation (curing). Rheology and mainly temperature modulated differential scanning calorimetry (TMDSC) have been used to investigate interactions between the silica nanoparticles and molecules of the epoxy oligomer or molecules of the growing epoxy network. Measurements of the complex specific heat capacity before curing showed that interactions between the nanoparticles and DGEBA molecules are very weak. An expression for an effective specific heat capacity of the silica nanoparticles could be deduced. Examination of the isothermal curing process after addition of an amine hardener yielded evidences for a restricted molecular mobility of the reactants in the cause of network formation. These restrictions could be overcome by increasing the curing temperature. No evidences for an incorporation of the silica nanoparticles into the epoxy network, i.e. for a strong chemical bonding to the network, were found. Interactions between the silica nanoparticles and the epoxy resins under study are assumed to be of a physical nature at all stages of network formation.

1. Introduction

Epoxy thermosets are nowadays widely used for technical applications such as adhesive joints or matrix materials in fiber-enforced plastics. Selective modification of epoxy matrices with filler particles has been successfully applied to adapt the materials to different physical, chemical or technical needs [1–9]. In recent years epoxy nanocomposites, i.e. epoxies filled with nanoscaled particles, have become more and more important because of their outstanding properties. The huge internal surfaces of the incorporated nanoparticles give rise to effects leading to novel macroscopic properties such as improved fracture toughness along with improved mechanical stiffness. A general understanding of the relationship between nanoscopic and macroscopic properties is still lacking. The aim of this work is to contribute to this subject by mainly exploiting dynamic investigations of thermal properties using temperature modulated differential scanning calorimetry (TMDSC).

The nanocomposites under study are mixtures of epoxies based on bisphenol-A with silica nanoparticles coated with a hydrophobic layer. This layer leads on one hand to an agglomerate-free dispersion of the nanoparticles inside the matrix and on the other hand ought to improve the bonding between nanoparticles and epoxy network [10–12].

Macroscopic properties of nanocomposites based on the same type of silica particles have been extensively studied by the workgroup of A.J. Kinloch [5,13–16]. Toughening mechanisms, tensile modulus and fracture toughness were examined by mechanical tests. This lead to the conclusion that the improved fracture toughness of these nanocomposites is caused by debonding of the nanoparticles and subsequent plastic void growth under load [13]. The strength or kind of the bonding of the nanoparticles to the epoxy was not in the focus of the studies. Thermal investigations presented in these works indicate that in fully cured thermosets the glass transition temperature measured by DSC or DMTA remains unchanged when silica nanoparticles are incorporated. In contrast to these results Rosso et al. [17] reported a dependency of the glass transition temperature on the concentration of nanoparticles. Amino-rich interphase regions around the nanoparticles were made responsible for a changed curing behaviour. Previous

* Corresponding author. Tel.: +352 466644 6755; fax: +352 466644 6329.
E-mail address: joerg.baller@uni.lu (J. Baller).

0032-3861/$ – see front matter © 2009 Elsevier Ltd. All rights reserved.
doi:10.1016/j.polymer.2009.05.020

investigations of epoxy resins filled with alumina (n-Al_2O_3) or silica nanoparticles (n-SiO_2) similar to the ones used throughout this study showed fundamental differences in the physical properties of these systems [18]: especially the glass transition behaviour is drastically changed by the incorporation of n-Al_2O_3 particles. For the latter systems, a study of the curing behaviour revealing the influence of interactions between epoxy molecules and alumina particles has recently been reported [19]. In the case of n-SiO_2 particles, no effect of the particles on the glass transition behaviour of the pure epoxy resins was found [18].

In this work we will mainly exploit dynamic thermal investigations to shed light onto the interactions between bisphenol-A based epoxies and silica nanoparticles. The nature of these interactions can be physical as well as chemical. We first present a more profound and extended analysis (compared to [18]) of epoxy resins filled with silica nanoparticles to investigate the interactions between the nanoparticles and the DGEBA oligomers. In a second step we investigate the curing behaviour of the corresponding epoxy nanocomposites by adding an amine hardener. Thermal investigations are supported by rheological measurements of the nanocomposites' curing behaviour.

2. Experimental

2.1. Materials and sample preparation

As previously mentioned this work is dealing with the examination of two different types of nanocomposites:

2.1.1. Resin nanocomposites

A master batch of diglycidyl ether of bisphenol-A (DGEBA) filled with 40 mass% of silica nanoparticles (Nanopox A410, nanoresins AG, Geesthacht, Germany) is the basis for all resin nanocomposites. This master batch was diluted with the same type of distilled DGEBA (nanoresins AG). We determined the Epoxy Equivalent Weight (EEW) of the nanocomposites for five different mass concentrations $x = m^{SiO_2}/(m^{DGEBA} + m^{SiO_2})$ by wet analysis (DIN EN ISO 3001, e.g. [20]). The term EEW is defined as the weight of material which contains one mol of epoxy groups [20]. Results are shown in Table 1.

The mean diameter of the silica nanoparticles is about 20 nm. This includes a silane layer from which nothing is published by nanoresins AG except its hydrophobic character. The particles have a narrow size distribution and are homogeneously distributed inside the oligomer matrix [4,13–16]. Due to the sol–gel fabrication process [21,22] and due to the silane layer, there is no aggregation of particles [4,13–16] (see also Fig. 1). According to the manufacturer, Nanopox A410 includes the same nanoparticles as the nanocomposites (e.g. Nanopox F400) described in Refs. [4,13–16].

2.1.2. Epoxy nanocomposites

Resin nanocomposites were cured using diethylene triamine (DETA) from Fluka Chem. as a hardener. A non-stoichiometric mass ratio of $s = 0.142 \pm 0.001$ between hardener and resin ($s = m_{hardener}/m_{resin}$) has been used for all measurements presented throughout this work. Resin and hardener mixed with this ratio are known to yield adhesives with maximum tensile shear strength during fracture experiments performed on different epoxy mixtures glued on native aluminium [23]. The error of about 0.7% in mixing ratio s is due to pipetting and was determined by weighing. Uncertainty in measured heat flow or heat capacity data of the epoxy nanocomposites is mainly attributed to this error.

Table 1
Epoxy equivalent weight measured by wet analysis of the resin nanocomposites for different mass concentrations x of nanoparticles.

x	EEW (g/mol)
0	181 ± 2
0.1	202 ± 2
0.2	226 ± 5
0.3	265 ± 1
0.4	295 ± 3

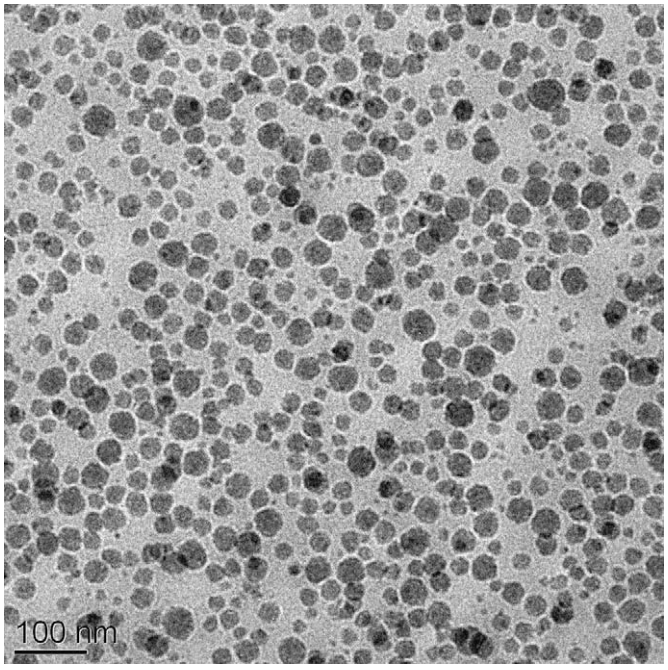

Fig. 1. TEM micrograph of an epoxy nanocomposite with 40 mass% of silica nanoparticles ($x = 0.4$).

The curing process was started by injecting the hardener into the resin nanocomposites. After stirring the mixtures (about one gram) by hand for five minutes at $T_{stir} = (298 \pm 1)$ K, they were isothermally cured inside a differential scanning calorimeter and inside a rheometer at $T_{cure} = 298$ K. To perform dynamic cure experiments samples were quenched to 278 K directly after mixing. On one hand, this temperature is low enough to significantly slow down the chemical processes for the resin/hardener combination used throughout this work thus avoiding loss of data at the start of the curing process. On the other hand this temperature is high enough to avoid condensation of water or formation of ice. Once inside the calorimeter the samples were further quenched to 240 K before the start of the dynamic cure experiments.

2.2. Calorimetric measurements

Thermal investigations were performed using temperature modulated differential scanning calorimetry (TMDSC) on a DSC823e and a modified [24,25] DSC821e (Mettler Toledo, Switzerland). The instruments were temperature and heat flow calibrated using water, indium, naphthalene and benzoic acid. Sample masses were between 15 and 25 mg.

In a TMDSC experiment the calorimeter furnace is controlled by the following temperature program

$$T(t) = T_0 + \beta t + T_a \sin \omega t \quad (1)$$

During the isothermal curing experiments, $T_0 = 298$ K, $\beta = 0$, the temperature amplitude was $T_a = 0.5$ K and the angular frequency $\omega = 2\pi/t_p = 0.052$ rad/s, $t_p = 120$ s representing the modulation period.

In the frame of linear response theory the heat flow Φ into the sample can be written as [28]:

$$\Phi = \Phi^{u} + \Phi^{a}\cos(\omega t - \varphi) \quad (2)$$

This signal can be deconvolved in order to get the underlying heat flow Φ^{u}, the amplitude Φ^{a} of the modulated heat flow and the phase angle φ between the measured heat flow and the temperature rate. Φ^{u} is related to the conventional DSC curve. In the case of an isothermal cure experiment Φ^{u} is proportional to the calorimetric reaction rate. The modulus of the specific complex heat capacity at constant pressure $|c_p^*|$ is determined from the respective amplitudes of the temperature T_a and the heat flow Φ^{a}

$$|c_p^*| = \frac{K\Phi^{a}}{mT_a\omega} \quad (3)$$

where m is the sample mass. The calibration factor K is obtained using an aluminum standard with well known specific heat capacity.

Fig. 2 shows $|c_p^*|$ and φ curves for the pure DGEBA resin. From this data real and imaginary part of the nanocomposites' heat capacity can be evaluated by using a standard method for TMDSC [26].

Calorimetric measurements of the curing process have been started about 6–8 min after injecting ($t_{cure} = 0$) the hardener into the resin nanocomposites. Measured data has been linearly extrapolated to $t_{cure} = 0$.

The calorimetric measurements have been carried out with a sampling rate of one data point per second. In most of the following figures, symbols are only used for the sake of clarity; data points lie much closer and are represented by solid line unless stated otherwise.

2.3. Rheological measurements

Steady shear flow curves $\tau(\dot{\gamma})$ have been recorded by means of a HAAKE MARS II rheometer [27] to determine the zero-shear viscosity $\eta_0 = d\tau/d\dot{\gamma}|_{\dot{\gamma}\to 0}$. We used plate–plate geometry with disposable alumina plates of a diameter of 20 mm and a gap of 1 mm. In order to avoid heating-up of the samples by the import of too large quantities of mechanical energy, the sweeping range of $\dot{\gamma}$ was continuously reduced as the reaction progressed. This method allows for keeping the curing temperature constant at $T_{cure} = (298.0 \pm 1)$ K. η_0 was obtained from the flow curves by extrapolating the lower Newtonian plateau to $\dot{\gamma} = 0$.

3. Results and discussion

3.1. Epoxy resins filled with silica nanoparticles

Measurement of the epoxy equivalent weight (EEW) by wet analysis is a quite simple but nevertheless promising approach to investigate the influence of filler materials on the reactivity of epoxy resins: if an oxirane ring (epoxy group) would have been opened by a chemical reaction with the filler material, it would no longer contribute to the EEW as determined by wet analysis [20]. Fig. 3 shows measured and calculated values for the EEW of the resin nanocomposites used throughout this study. The calculated data were determined for $x > 0$ from the measured EEW of the pure resin ($x = 0$) under the assumption that the SiO_2 part has no influence on the reactivity of the epoxy rings:

$$EEW_{calc}(x) = \frac{EEW_{meas}(x = 0)}{(1 - x)} \quad (4)$$

Fig. 3 shows that calculated and measured EEW data coincide for all concentrations x within the margin of experimental error. This leads to the conclusion that the silica nanoparticles have no influence on the reactivity of the functional groups (oxirane rings) in the nanocomposite resins.

Investigation of dynamic properties of oligomer molecules inside the nanocomposite resins is a method to get hints for interactions between matrix molecules and nanoparticle fillers: any physical or chemical interaction between DGEBA oligomer molecules and n-SiO_2 particles will influence the molecular dynamics of the oligomer matrix. The part of the dynamics which is responsible for the intrinsic structural relaxation process (α process) is expected to be changed by interactions at the surface of the silica nanoparticles. Due to the enormous surface of the n-SiO_2 particles inside the composites, the modification of the dynamics should be clearly visible by investigating the α process as a function of nanoparticle content. In calorimetry, the α process can be examined by measuring the complex specific heat capacity with TMDSC [28]. Due to the restricted frequency range of classical TMDSC, these investigations have been done in the temperature regime at a given fixed frequency rather than as a function of probe frequency. The α process can then be studied by examining the temperature dependences of the real and imaginary part of the complex specific heat capacity in the vicinity of the dynamic glass transition [28]. Due to the low frequency of 8 mHz used for this

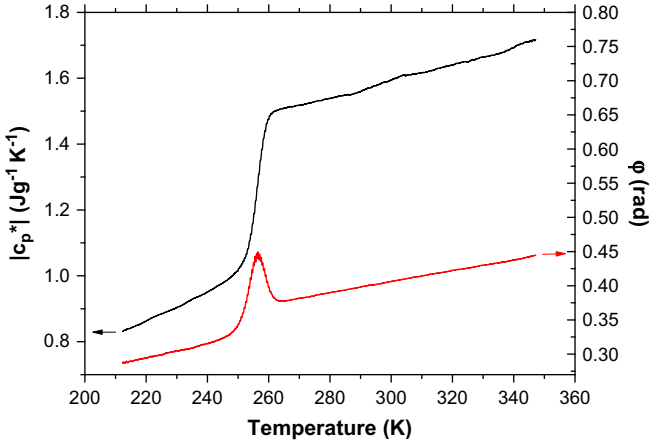

Fig. 2. Modulus of the specific heat capacity and phase angle of DGEBA according to (2) and (3). $\beta = 0.5$ K/min, $T_a = 0.5$ K, $t_p = 120$ s.

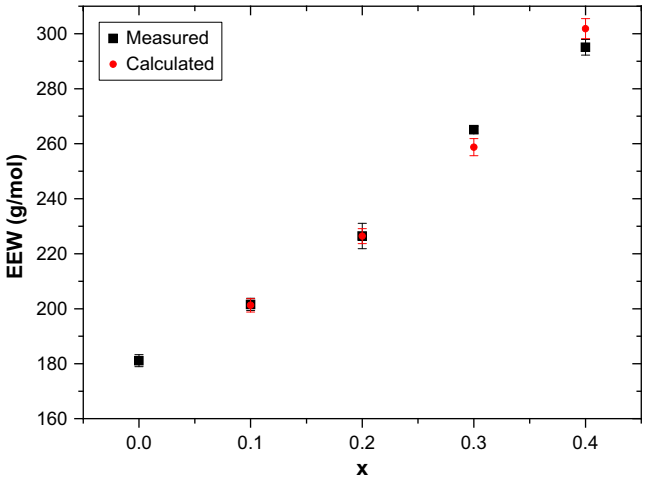

Fig. 3. Epoxy equivalent weight of the resin nanocomposites as a function of particle concentration x.

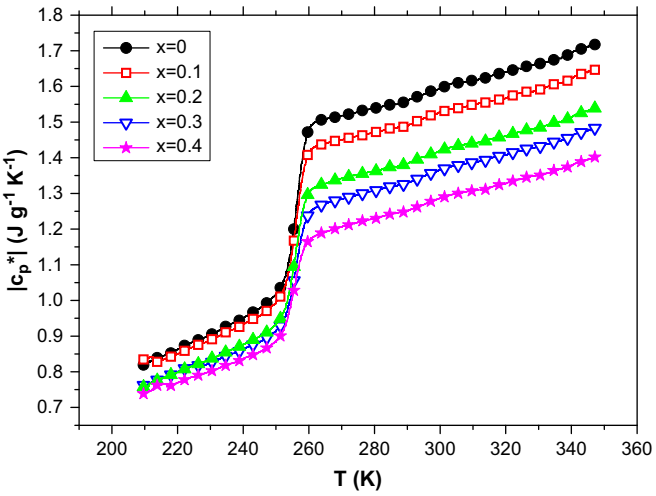

Fig. 4. Modulus of the complex specific heat capacity of the resin nanocomposites for different mass concentrations x of n-SiO_2. $\beta = 0.5$ K/min, $T_a = 0.5$ K, $t_p = 120$ s.

study the dynamic glass transition temperature lies near the thermal glass transition temperature.

In a first set of measurements, we examined the influence of the n-SiO_2 particles onto the thermal properties of the pure resin. Fig. 4 shows the modulus of the complex specific heat capacity $|c_p^*|$ of the DGEBA resins filled with different amounts of SiO_2 nanoparticles.

The corresponding c_p''-curves are shown in Fig. 5. These results agree well with prior studies on similar silica nanocomposite systems [18]. In the following we tried to separate the respective contribution of the pure resin to the measured heat capacities from the one of the silica nanoparticles. Real and imaginary part of the pure epoxy resin's specific heat capacity was calculated by two different ways:

a) Imaginary part of the specific heat capacity

The non-zero imaginary parts of the specific heat capacities of the nanocomposites stem from the resin part of the composite: only the oligomer molecules are expected to show relaxation behaviour around the thermal glass transition. The n-SiO_2 part should not contribute to the imaginary part of the composites'

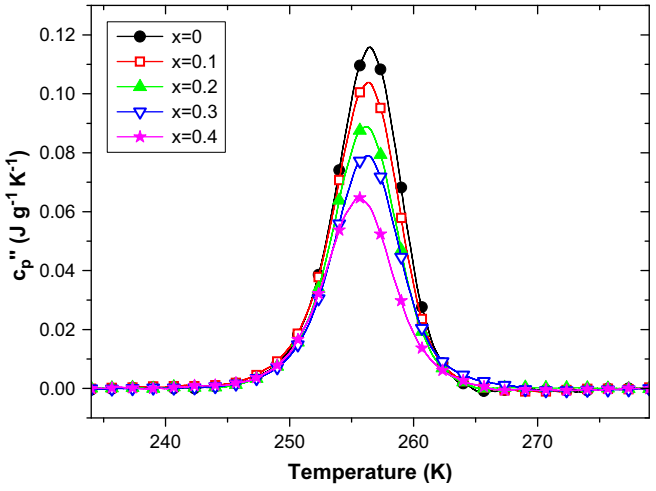

Fig. 5. Imaginary part of the specific heat capacity of the resin nanocomposites for different mass concentrations x of n-SiO_2 particles. $\beta = 0.5$ K/min, $T_a = 0.5$ K, $t_p = 120$ s.

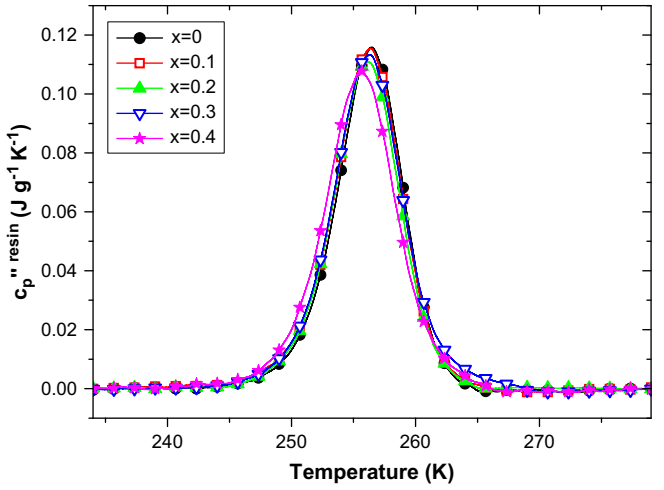

Fig. 6. Imaginary part of the heat capacity per gram DGEBA of the resin nanocomposites for different mass concentrations of n-SiO_2 particles. $\beta = 0.5$ K/min, $T_a = 0.5$ K, $t_p = 120$ s.

overall heat capacities. It is well understood that the n-SiO_2 particles can strongly influence the relaxation behaviour of the oligomer molecules if there exists a significant interaction between the oligomer molecules and the fillers – especially because of the nanoparticles' enormous surface. To shed light onto this influence, we apply a simple mixing rule to "correct" the c_p''-data as if both components of the nanocomposite did not interact (Fig. 6, Table 2):

$$c_p''^{\text{resin}} = \frac{|c_p^*|\sin(\varphi)}{(1-x)} = \frac{c_p''}{(1-x)} \tag{5}$$

The data represented in Fig. 6 and Table 2 lead to the conclusion that the dynamic glass transition behaviour of the epoxy resins as revealed by TMDSC is only slightly affected by the presence of the n-SiO_2 particles: the glass transition temperature T_g decreases only by 0.7 K by the incorporation of n-SiO_2 particles with up to 40 weight percent. The area of the c_p''-peak remains constant, which means that the number of relaxators per gram matrix which take part in the relaxation process and their relaxation strength remain the same. This is an important result because it means that there is no tight sticking or bonding of oligomer molecules to the nanoparticles.

The shape of the c_p''-peak is slightly changed to a wider (referred to temperature) and flatter distribution of relaxators. These changes are nevertheless very small taking the enormous surface (see above) of the n-SiO_2 particles into account. This suggests that the hypothesis of independent components which is implied by the use of equation (5) seems to hold true.

b) Real part of the specific heat capacity

The validity of a mixing rule (5) for c_p'' leads to the question if a similar rule for the real part of the specific heat capacity can be

Table 2
Characteristic data of the dynamic glass transition of the resin nanocomposites. Data corrected for the resin part (see text).

x	$c_p''^{\text{resin}}$ peak				$c_p'^{\text{resin}}$
	T_g^{dyn} (K)	Area (J g^{-1})	Width (K)	Height (J g^{-1} K^{-1})	Δc_p (J g^{-1} K^{-1})
0	256.3	0.76	5.35	0.123	0.49
0.1	256.2	0.77	5.47	0.122	0.49
0.2	256.0	0.74	5.44	0.117	0.50
0.3	256.1	0.79	5.72	0.119	0.49
0.4	255.6	0.77	5.86	0.114	0.50

found. In contrast to c''_p, the situation is more complex for c'_p: the heat capacity of the nanoparticles has to be taken into account. Since we have no means to measure the unknown specific heat capacity of n-SiO_2, the $|c^*_p|$-curves of Fig. 4 have been used to calculate an effective specific heat capacity $c^{SiO_2}_{p_{eff}}(T)$ of the silica particles inside the resins by using the following procedure: from the curves with $x \neq 0$, the curve with $x = 0$ (without n-SiO_2) is subtracted according to the respective part of epoxy resin. This leads to four curves which nearly coincide and which represent an approximation for the nanoparticles' specific heat capacity under the assumption that a simple mixing rule for the heat capacities holds true (same working hypothesis as for c''_p). $c^{SiO_2}_{p_{eff}}(T)$ is then calculated by averaging these four data sets. The temperature dependence of $c^{SiO_2}_{p_{eff}}$ being known, we apply a similar mixing rule such as (5) to calculate the real parts of the heat capacities per gram resin:

$$c'^{resin}_p = \frac{|c^*_p|\cos(\varphi) - x c^{SiO_2}_{p_{eff}}}{(1-x)} = \frac{c'_p - x c^{SiO_2}_{p_{eff}}}{(1-x)} \quad (6)$$

The results of these calculations can be seen in Fig. 7. The temperature dependence of $c^{SiO_2}_{p_{eff}}$ is shown as a dashed line. For $T = 293$ K the value of $c^{SiO_2}_{p_{eff}} = 0.80\ J\,g^{-1}\,K^{-1}$ lies relatively near to the one of silica glass ($0.73\ J\,g^{-1}\,K^{-1}$) or silica crystal ($0.75\ J\,g^{-1}\,K^{-1}$) found in literature [29].

From the description of the n-SiO_2 particles (see Section 2.1) it is not astonishing that these values do not exactly coincide – the nature of the n-SiO_2 particles (crystalline or amorphous) as well as influences of their coating onto the specific heat capacity is unknown. Nevertheless the use of the $c^{SiO_2}_{p_{eff}}(T)$ curve allows us to calculate the modulus of the complex heat capacity per gram resin.

As a result the glass transition behaviour as seen by TMDSC is not changed by the incorporation of silica nanoparticles. This again leads to the interpretation that the interaction between the oligomer molecules and the n-SiO_2 particles is weak. Concerning the specific heat capacity around the thermal glass transition, both components of the nanocomposites seem to behave independently.

As a first conclusion, the investigations of the resin nanocomposites do not yield evidences for a significant influence of the n-SiO_2 particles onto the macroscopic thermal behaviour of the DGEBA epoxy resin. Local interactions at the surfaces of the nanoparticles cannot be excluded but are supposed to be negligible. Furthermore there are no evidences for spatial restrictions for the oligomer molecules in the space between the silica nanoparticles.

It should finally be emphasized that we were able to deduce an expression for the specific heat capacity of the embedded nanoparticles from specific heat capacity measurements of nanocomposites with different filler concentrations.

3.2. Isothermal and dynamic curing of epoxy resins filled with silica nanoparticles

In the following the influence of the n-SiO_2 particles onto the curing process will be discussed. Determination of the epoxy equivalent weight has shown that the nanoparticles do not influence the reactivity of the oxirane rings. Furthermore, from the preceding section we have concluded that the interaction between resin oligomers and nanoparticles is weak. During curing the situation is completely different: there is a third component, the hardener, which comes into play.

The reaction of DGEBA resins with amino hardeners has been studied in detail [30–32] but there is nothing known about a possible physical or chemical interaction of the hardener with the n-SiO_2 particles. Due to the fact that the n-SiO_2 particles are only available inside the DGEBA resins (see Section 2.1), we have not been able to investigate this two-component interaction. The nanoparticles might also interact with the growing epoxy network – chemically or physically. In addition, effects like phase separation [32] – eventually caused or enforced by the n-SiO_2 particles – and reactions between the epoxy network and n-SiO_2 particles can play a role e.g. by contributing to the heat flow during curing.

To investigate this situation, isothermal curing experiments at 298 K have been performed by TMDSC. Fig. 8 shows the heat flows Φ^{epoxy} per gram epoxy (DGEBA and DETA) during curing of the nanocomposites. These data have been calculated from the underlying heat flow Φ^u (equation (2), "conventional" DSC signal) by using the following formula:

$$\Phi^{epoxy} = \frac{(s - xs + 1)\Phi^u}{s(1-x) + 1 - x} \quad (7)$$

with s being the ratio between hardener and resin: $s = m_{hardener}/m_{resin}$. To avoid the influence of different DSC baselines on the Φ^{epoxy}-curves for different concentrations of n-SiO_2

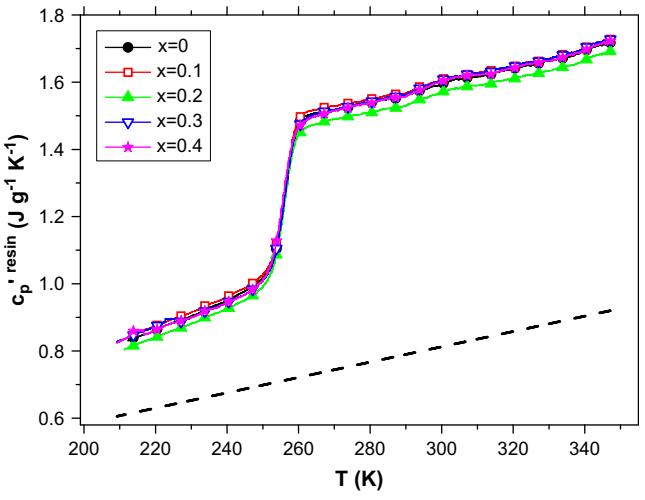

Fig. 7. Real part of the specific heat capacity of the resin nanocomposites for different mass concentrations of n-SiO_2 particles. Data corrected for the resin part (see text). Dashed line: $c^{SiO_2}_{p_{eff}}(T)$.

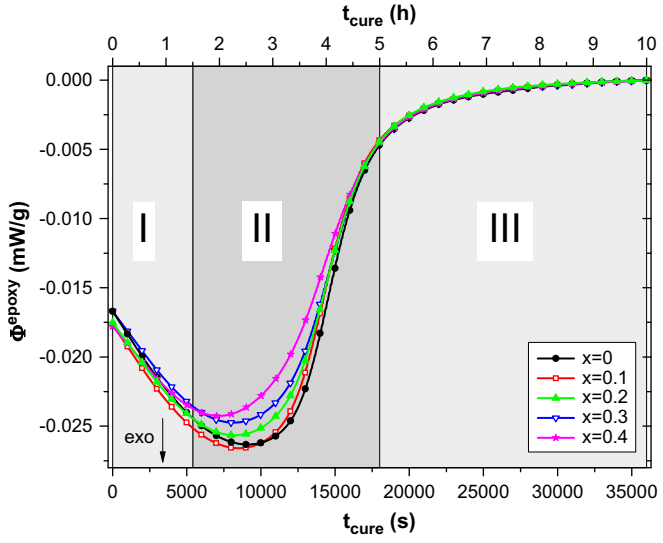

Fig. 8. Heat flow per gram epoxy during isothermal curing at 298 K.

particles, Φ^{epoxy}-curves have been slightly shifted vertically to give $\Phi^{epoxy} = 0$ for $t_{cure} = 36\,000$ s. This data treatment is justified by the fact that all heat flow curves are almost horizontal and even more important have the same slope at $t_{cure} = 36\,000$ s. The correction using equation (7) again expresses the working hypothesis that the nanocomposites consist of components which can be treated as being independent, i.e. only the epoxy part (resin plus hardener) of the nanocomposites is assumed to produce heat during isothermal curing.

The heat flow curves can be divided into three different regimes I to III (see Fig. 8):

At the beginning of the curing process (regime I), the reaction rate is the same for all concentrations of nanoparticles within the margin of experimental error (compare Fig. 9a). This means that there is no catalytic effect of the nanoparticles visible as recently found in alumina/epoxy nanocomposites [19]. This can be explained by the hydrophobic coating of the n-SiO_2 particles: a catalytic effect of –OH groups or of absorbed water on the nanoparticles' surfaces can be excluded. Beside the lack of an accelerating effect, the nanoparticles do not reduce the speed of reaction in regime I. This means that the generation of linear molecules which predominantly takes place at this stage of the curing process is not hindered [19] by the presence of the nanoparticles. This goes in line with the results presented in Section 3.1 for the resin nanocomposites: even at high filler contents the size of the network fragments formed in regime I is still small compared to the space between the nanoparticles.

After a curing time of about one and a half hour (regime II), the heat flow curves systematically split up: the higher the nanoparticles concentration, the lower the heat flow up to a curing time of about five hours. This slowing down of the chemical reaction by the nanoparticles is also reflected by the point in curing time of highest heat flow $t_{\Phi_{max}}$ (Fig. 9b): $t_{\Phi_{max}}$ systematically decreases with increasing nanoparticles concentration.

At the end of the curing process (regime III), after a curing time of about 5 h, the heat flow curves coincide again, leading to similar chemical reaction rates.

The described behaviour of the heat flow curves leads to a systematic dependency of the integrated heat of reaction per gram epoxy during isothermal cure at 298 K on the nanoparticles concentration (Table 3, Fig. 11): ΔH^{iso}_{epoxy} decreases by 8% from the pure epoxy system ($x = 0$) to the system filled with 40 mass percent of n-SiO_2 particles.

Table 3
Specific reaction heats during isothermal (ΔH^{iso}_{epoxy}) and dynamic (ΔH^{dyn}_{epoxy}) cure experiments. $\alpha_0(t_{cure} = 10\text{ h})$: conversions after 10 h of isothermal cure, calculated using the proper total specific reaction heat $\Delta H^{dyn}_{epoxy}(x)$ produced by each nanocomposite. $\alpha_0(t_{cure} = 10\text{ h})$: conversions after 10 h of isothermal cure calculated with respect to the total specific reaction heat $\Delta H^{dyn}_{epoxy}(0)$ of the epoxy without fillers. α_{dyn}: conversions after dynamic curing (see text).

x	ΔH^{iso}_{epoxy} (J/g)	ΔH^{dyn}_{epoxy} (J/g)	$\alpha(t_{cure} = 10\text{ h})$	$\alpha_0(t_{cure} = 10\text{ h})$	α_{dyn}
0	387	601	0.64	0.64	1
0.1	385	595	0.65	0.64	0.99
0.2	375	592	0.63	0.62	0.99
0.3	365	585	0.62	0.60	0.97
0.4	355	587	0.60	0.58	0.98

In addition to the isothermal curing we performed dynamic cure experiments by conventional DSC between 240 K and 450 K at a rate of 3 K/min to determine the total heat of reaction ΔH^{dyn}_{epoxy} for each system (Fig. 10, Table 3). Fig. 10 gives no hint for a significant impact of the nanoparticles on the chemical reaction during dynamic curing. This is in keeping with the results found for regime I of the isothermal cure experiment. Moreover the difference in specific reaction heat between $x = 0$ and $x = 0.4$ reduces from 8% during isothermal cure to less than 3% for the dynamic cure experiment (Fig. 11, Table 3). This means that part of the chemical reaction which does not take place during isothermal cure can be thermally activated by increasing the curing temperature. This is a strong hint for the interpretation that the interaction between the nanoparticles and the growing epoxy network or the reactants is weak. This does not exclude an influence of the nanoparticles on the mobility of the other components during the chemical reaction as will be seen in the following. It simply means that mobility restrictions due to the nanoparticles can be compensated by increasing the temperature and thus the thermal energy.

Measurement of the total specific reaction heat ΔH^{dyn}_{epoxy} by dynamic cure experiments allows for calculating the caloric conversion $\alpha(t)$ as a function of curing time during the isothermal experiments (Fig. 12):

$$\alpha(t) = \frac{\int_0^t \Phi^{epoxy}(t')\mathrm{d}t'}{\Delta H^{dyn}_{epoxy}} \qquad (8)$$

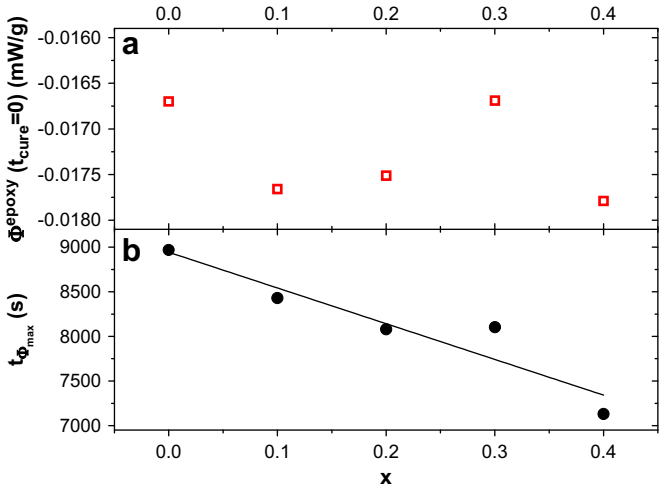

Fig. 9. (a) Heat flow per gram epoxy at the start of the curing process $\Phi^{epoxy}(t_{cure} = 0)$ (squares) for different mass concentrations x of filler particles. (b) Point in curing time of highest heat flow $t_{\Phi_{max}}$ (circles). The solid line serves as a guideline for the eyes.

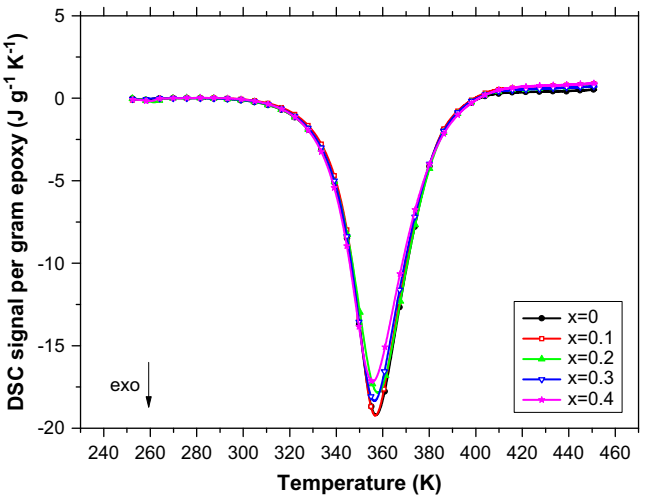

Fig. 10. DSC signals obtained from dynamic scans performed at a heating rate of 3 K/min. The data are corrected to the epoxy content of the composites.

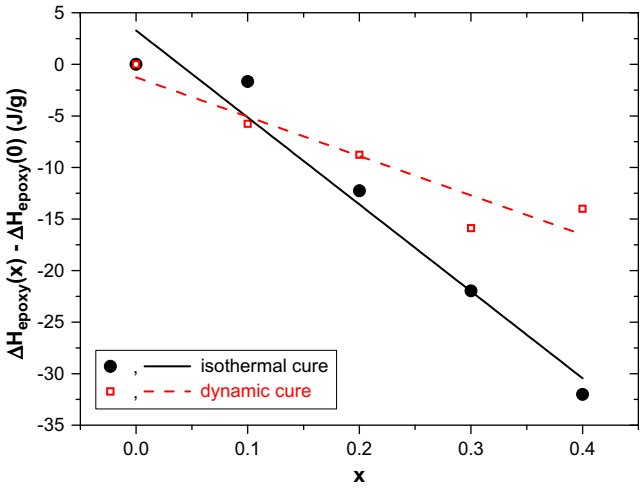

Fig. 11. Change of specific reaction heats (see Table 3) as a function of filler concentration x for both isothermal and dynamic cure experiments.

As already suggested by the temporal evolution of Φ^{epoxy} (Fig. 8, regime I), the conversion curves nearly coincide at early stages of the curing process. At the end of the isothermal experiment, there remains a difference in caloric conversion $\alpha(t_{\text{cure}} = 10\text{ h})$ (Table 3) with respect to the filler content x. To compare the final conversions $\alpha(t_{\text{cure}} = 10\text{ h})$ with the one of the system without nanoparticles, we replace $\Delta H^{\text{dyn}}_{\text{epoxy}}$ by $\Delta H^{\text{dyn}}_{\text{epoxy}}(0)$ in the denominator of (8). This leads to the values $\alpha_0(t_{\text{cure}} = 10\text{ h})$ in Table 3 which indicate that during isothermal cure, the filled systems react less than the neat epoxy. If we want to do the same comparison of conversions for dynamic cure experiments we have to modify (8):

$$\alpha_{\text{dyn}} = \frac{\Delta H^{\text{dyn}}_{\text{epoxy}}(x)}{\Delta H^{\text{dyn}}_{\text{epoxy}}(0)} \tag{9}$$

The values of α_{dyn} given in Table 3 vary only by 2% as a function of the filler content. This again reflects the fact, that the missing heat of reaction of filled systems compared to the neat epoxy can be released by thermal activation during dynamic cure experiments.

Numerical derivation of the $\alpha(t)$ curves yields the reaction rates $d\alpha/dt$. The reactions rates are modelled by semi-empirical Kamal equations taking into account autocatalytic nth order kinetics [33]:

$$\left(\frac{d\alpha}{dt}\right)_{\text{chem}} = (k_1 + k_2\alpha^m)(1-\alpha)^n \tag{10}$$

k_1 and k_2 are temperature-dependent rate constants; m and n represent empirical reaction parameters. The result of these calculations can be seen in Fig. 13.

In the chemically controlled regime the $d\alpha/dt$ – curves of all the investigated samples can be fitted to the Kamal model (equation (10)). The deviation of $d\alpha/dt$ from the Kamal model $(d\alpha/dt)_{\text{chem}}$ reflects the transition to a regime where the evolution of $d\alpha/dt$ no longer can be described solely by autocatalytic nth order kinetics. This deviation is usually attributed to mobility restrictions inside the network and marks the transition from the chemically to the diffusion controlled regime of the respective reaction [33]. As a first result, Fig. 13 shows that the nature of the chemical reaction (autocatalytic nth order kinetics) is not changed by the incorporation of silica nanoparticles.

The coincidence of the heat flow curves at early curing times (Fig. 8) is reflected by the coincidence of the reaction rates at low conversions (Fig. 13). To further investigate the beginning of the isothermal curing process and the transition to regime II, we performed measurements of the zero-shear viscosity during isothermal cure at 298 K (Fig. 14). At an early curing stage, η_0 is in the same order of magnitude for all concentrations.

The transition to regime II (Fig. 8) is also marked by a change in Fig. 14: the η_0 curves no longer coincide; the higher the filler concentration x the earlier they start to diverge from the (nearly) horizontal course at the beginning. An operative percolation time t_{opgel} has been estimated (Table 4) by extrapolating $\eta_0^{-1}(t)$ linearly to zero in the final stage of the isothermal experiment [34]. Although the method lacks of accuracy [34], Table 4 suggests that t_{opgel} depends on the concentration of the nanoparticles. The increase of the zero-shear viscosity η_0 can have different reasons:

(a) It is well known from literature that the zero-shear viscosity η_0 increases with the mass average molecular mass of the molecules in the course of polymer network formation. From

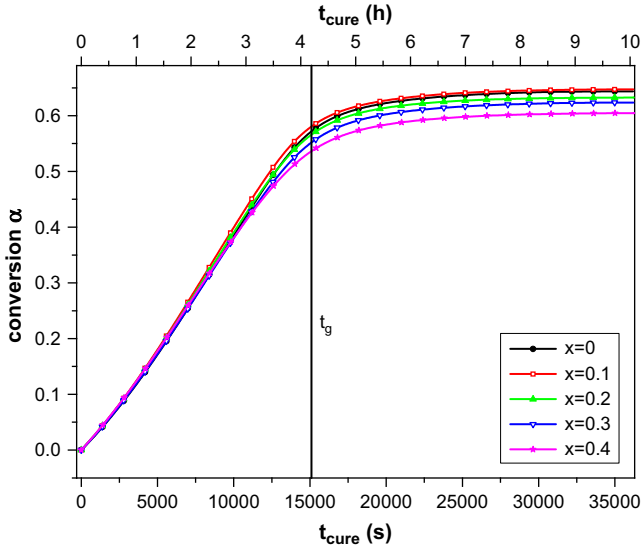

Fig. 12. Calorimetric conversion as a function of curing time. Conversions are calculated using the proper total reaction heat produced by each nanocomposite. t_g gives the point in time of the dynamic glass transition as seen by the inflection points of the c_p curves in Fig. 15.

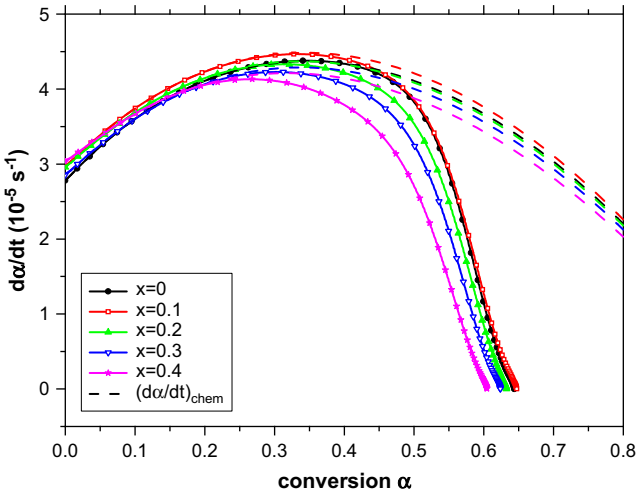

Fig. 13. Reaction rates as a function of calorimetric conversion. The dashed lines represent the chemical conversion rates and correspond to fits of the experimental data to the Kamal model (10).

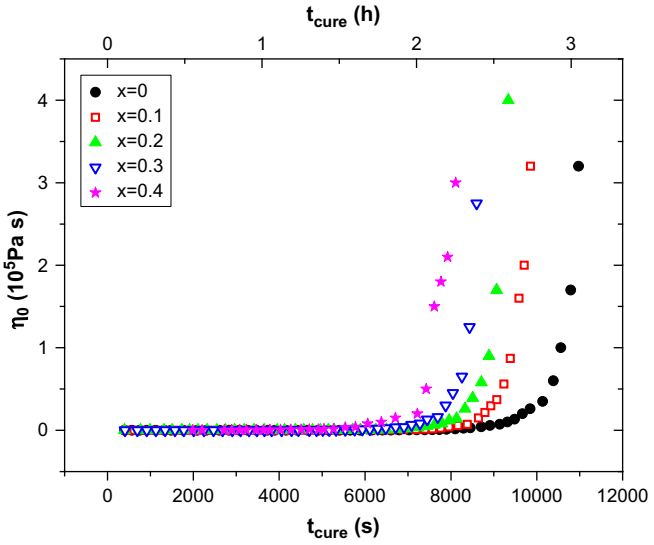

Fig. 14. Zero-shear viscosity as a function of curing time during isothermal curing at 298 K for different particle concentrations x.

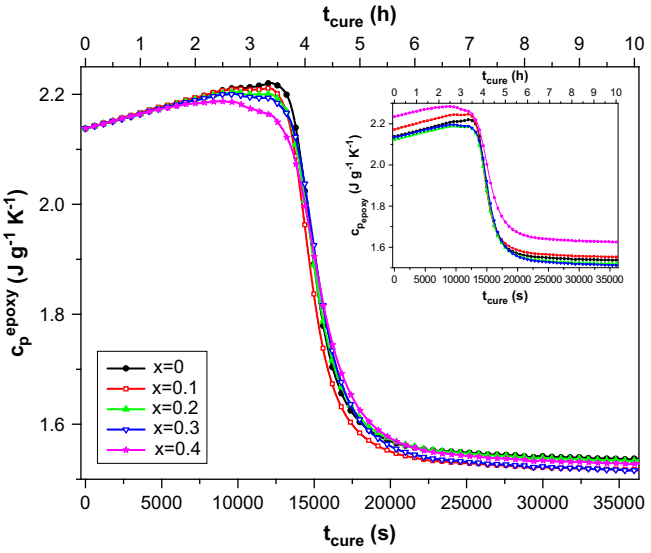

Fig. 15. Specific heat capacity per gram epoxy c_p^{epoxy} during isothermal cure. Curves have been shifted together at $t_{cure} = 0$ (see text). Inset: c_p^{epoxy} before shift.

the heat flow and conversion curves (Figs. 8 and 12) we concluded that there is no catalytic effect of the nanoparticles on the chemical reaction. This means that an earlier increase of the mass average molecular mass for filled composites should not be attributed to an accelerated network formation by a catalyzed reaction but to an incorporation of nanoparticles into the epoxy network.

(b) The zero-shear viscosity η_0 generally increases when the mobility is reduced. If the time evolution of the mobility restrictions depends on the concentration of the filler particles, then there exists an interaction between fillers and matrix material. The difference to (a) consists in the strength of the interaction: it can be purely physical, i.e. the nanoparticles are not chemically bonded to the epoxy network but are the cause of mobility restrictions.

The fact that the total specific heat of reaction per gram epoxy ΔH_{epoxy}^{dyn} remains almost constant for all concentrations x supports the idea that the interaction between nanoparticles and matrix is physical (scenario (b) or scenario (a)) with weak interaction forces. Of course it cannot be completely excluded that there exists a chemical interaction which does not significantly affect calorimetric properties.

Fig. 15 shows the temporal evolution of the specific heat capacity during isothermal curing. The curves have been retrieved from the same measurements as before (Fig. 8) by exploiting (3) and a modified form of (6) to take the hardener content into account:

$$c_p^{epoxy} = \frac{(s - xs + 1)c_p - x c_{p_{eff}}^{SiO_2}}{s(1-x) + 1 - x} \tag{11}$$

Despite these corrections the difference of the absolute values is below 5% (see inset in Fig. 15) which is the precision of c_p data usually given in literature. It should be stressed that this is again a sign for the validity of the determination of $c_{p_{eff}}^{SiO_2}$ in Section 3.1. To better compare the temporal evolution of the specific heat capacities c_p^{epoxy}, the curves have been laid together at $t_{cure} = 0$ (Fig. 15) [19].

The higher the nanoparticle concentration the lower is the slope of the c_p^{epoxy} curves just before the dynamic glass transition. The increase of c_p^{epoxy} at early curing times has been explained by entropy production due to the chemical reaction [35–37]. That means that if the chemical reaction slows down, the slope of c_p^{epoxy} should decrease. Comparison of Figs. 8 and 15 shows that indeed both effects start at about the same point in time.

The most prominent feature of the c_p^{epoxy} curves is the point in time $t_g = 15100 \pm 400$ s of the chemical glass transition (determined by the inflection points in Fig. 15). Within the experimental error, there exists no dependency of t_g on the filler concentration x. This can be explained by an opposite influence of two processes during cure:

On one hand there is a slowing down of the chemical reaction by increased mobility restrictions. This should lead to a longer-lasting chemical reaction. On the other hand, the increasing immobility leads to the occurrence of the chemical glass transition at lower conversions (see Fig. 12). Both effects superpose and as a consequence at a late curing stage, the heat flow curves merge and the glass transition occurs at the same time for all concentrations. At first sight, the unchanged t_g seems to be in contradiction to the results presented by Rosso et al. [17]. We attribute this discrepancy to the different types of hardener used for both studies.

This picture is also supported by a closer look at the reaction rates (Fig. 13): the influence of the loss of molecular mobility on the reaction kinetics can be described by a diffusion factor [38] defined as

$$DF(t) = \frac{\frac{d\alpha}{dt}}{\left(\frac{d\alpha}{dt}\right)_{chem}} \tag{12}$$

As long as the nanocomposites evolve in the chemically controlled regime, the diffusion factor equals one. When molecular mobility restrictions become significant the reactions progress in the diffusion controlled regime and DF < 1 [38]. Fig. 16 shows how the diffusion factors of the investigated nanocomposites evolve as

Table 4
t_{opgel} for different mass concentrations x of nanoparticles.

x	t_{opgel} (s)
0	11 200
0.1	10 100
0.2	9400
0.3	8700
0.4	8600

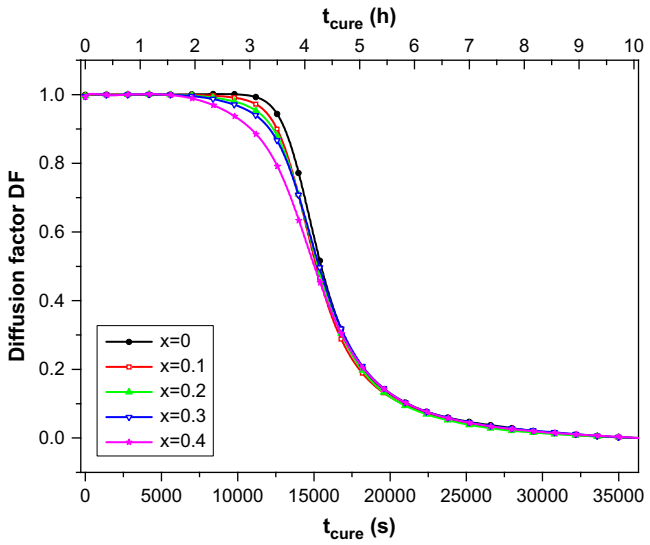

Fig. 16. Diffusion factor as a function of curing time.

a function of curing time. The diffusion factor curves show a similar behaviour as the c_p^{epoxy} curves despite the fact that they have different origins (heat of reaction vs. thermodynamic susceptibility). The DF curves start to separate at the transition from regime I to regime II (see also Fig. 8). This means the higher the nanoparticle concentration the higher the mobility restrictions from this time on. At the transition to regime III, the curves coincide again, leading to the experimental fact that the chemical glass transition occurs at the same point in time for all nanoparticle concentrations. At t_g, the mobility as measured by the diffusion factor becomes the same but the structure of the nanocomposites differs depending on the filler concentration because of the different conversions at this point in time (Fig. 12).

4. Conclusions

Epoxy resins filled with silica particles have been investigated before and during cure. Investigation of the thermal properties of the nanocomposites before curing has lead to an expression for the specific heat capacity of the particles themselves. In the first stage of isothermal curing, the presented measurements show no influence of the nanoparticles on the curing process. Afterwards there are mobility restrictions caused by the nanoparticles. One possible explanation for this could be that at the beginning of the curing there is formation of network fragments all over the sample. After a certain time, the size of these network fragments reaches the typical distances between the nanoparticles. Starting at this point in time, the mobility of the matrix is restricted. This leads on one hand to a reduced reaction rate as can be seen by the heat flow data and on the other hand to a reduction of the configurationally degrees of freedom reflected by the evolution of the specific heat capacity. The concurrence of these two effects is made responsible for the result that the point in time of the chemical glass transition during isothermal cure is independent of the filler content.

Despite the fact that hydrophobic coatings are often used to improve the bonding between filler particles and epoxy matrix [10], we come to the conclusion that the interaction between coated silica nanoparticles and epoxy matrix is relatively weak (physical) at all stages of cure for the nanocomposites under study. This does not necessarily affect the efficiency of fracture toughening of cured nanocomposites: a strong (chemical) bond is no prerequisite for the interpretation of the improvement of the mechanical properties as given in Ref. [13].

Acknowledgment

This work was kindly supported by the University of Luxembourg and the Ministère de la Culture, de l'Enseignement Supérieur et de la Recherche du Grand-Duché du Luxembourg.

References

[1] Wetzel B, Haupert F, Zhang MQ. Composites Science and Technology 2003;63:2055.
[2] Ji QL, Zhang MQ, Rong MZ, Wetzel B, Friedrich K. Journal of Materials Science 2004;39:6487.
[3] Han JT, Cho K. Journal of Materials Science 2006;41:4239.
[4] Kinloch AJ, Taylor AC. Journal of Materials Science 2006;41:3271.
[5] Kinloch AJ, Masania K, Taylor AC, Sprenger S, Egan D. Journal of Materials Science 2008;43:1151.
[6] Dudkin BN, Zainullin GG, Krivoshapkin PV, Krivoshapkina EF, Ryazanov MA. Glass Physics and Chemistry 2008;34:187.
[7] Zhang H, Zhang Z, Friedrich K, Eger C. Acta Materialia 2006;54:1833.
[8] Zhai LL, Ling GP, Wang YW. International Journal of Adhesion & Adhesives 2007;28:23.
[9] Gorbatkina YA, Ivanova-Mumzhieva VG, Ul'yanova TM. Polymer Science Series C 2007;49:131.
[10] Sreekala MS, Eger C. In: Friedrich K, Fakirov S, Zhang Z, editors. Polymer composites. New York: Springer; 2005. p. 91–105.
[11] Kitey R, Tippur HV. Acta Materialia 2005;53:1153.
[12] Kitey R, Tippur HV. Acta Materialia 2005;53:1167.
[13] Johnsen BB, Kinloch AJ, Mohammed RD, Taylor AC, Sprenger S. Polymer 2007;48:530.
[14] Kinloch AJ, Taylor AC, Lee JH, Sprenger S, Eger C, Egan DJ. Journal of Adhesion 2003;79:867.
[15] Kinloch AJ, Mohammed RD, Taylor AC, Eger C, Sprenger S, Egan D. Journal of Materials Science 2005;40:5083.
[16] Blackman BRK, Kinloch AJ, Sohn Lee J, Taylor AC, Agarwal R, Schueneman G, et al. Journal of Materials Science 2007;42:7049.
[17] Rosso P, Ye L. Macromolecular Rapid Communication 2007;28:121.
[18] Sanctuary R, Baller J, Krüger JK, Schaefer D, Bactavatchalou R, Wetzel B, et al. Thermochimica Acta 2006;445:111.
[19] Sanctuary R, Baller J, Zielinski B, Becker N, Krüger JK, Philipp M, et al. Journal of Physics: Condensed Matter 2009;21:035118.
[20] Lee H, Neville K. Handbook of epoxy resins. New York: McGraw-Hill; 1967.
[21] Sprenger S, Eger C, Kinloch AJ, Taylor AC, Lee JH, Egan D. Adhäsion Kleben Dichten 2003;3:24e8.
[22] Hanse Chemie. Patent Application WO 02/083776 A1; 2002.
[23] Possart W, editor. Adhesion, current research and applications. Weinheim: Wiley; 2005.
[24] Krüger JK, Bohn K, le Coutre A, Mesquida P. Measurement Science and Technology 1998;9:1866.
[25] Mesquida P, le Coutre A, Krüger JK. Thermochimica Acta 1999;330:137.
[26] Weyer S, Hensel A, Schick C. Thermochimica Acta 1997;305:267.
[27] Halley PJ, Mackay ME. Polymer Engineering and Science 1996;36:593.
[28] Schawe JEK. Thermochimica Acta 1995;260:1.
[29] Blachnik R. D'Ans-Lax Taschenbuch für Chemiker und Physiker. 4th ed. Berlin: Springer; 1998. p. 945.
[30] Habenicht G. Kleben. 5th ed. Berlin, Heidelberg, New York: Springer; 2006. p. 77.
[31] Ellis B. Introduction to the chemistry, synthesis, manufacture and characterization of epoxy resins. In: Ellis B, editor. Chemistry and technology of epoxy resins. London: Blackie Academic & Professional; 1993.
[32] Drzal LT. The interphase in epoxy composites. In: Dusek K, editor. Epoxy resins and composites. 2nd ed. Berlin, Heidelberg: Springer; 1986.
[33] Kamal MR. Polymer Engineering and Science 1974;14:231.
[34] Malkin AY, Kulichikhin SG. Advances in Polymer Sciences 1991;101:217.
[35] Schawe JEK, Alig I. Colloid Polymer Science 2001;279:1169.
[36] Ferrari C, Salvetti G, Tombari E, Johari GP. Physical Review E 1996;54:1058.
[37] Viciosa MT, Hoyo JQ, Dionisio M, Ribelles JL. Journal of Thermal Analysis and Calorimetry 2007;90:407.
[38] Van Assche G, Van Hemelrijck A, Rahier H, Van Mele B. Thermochimica Acta 1995;268:121.